ACS central science

http://pubs.acs.org/journal/acscii

Research Article

High-Content Imaging Platform to Discover Chemical Modulators of Plasma Membrane Rafts

Nico Fricke,[¶] Krishnan Raghunathan,[¶] Ajit Tiwari,[¶] Katherine M. Stefanski, Muthuraj Balakrishnan, Alex G. Waterson, Ricardo Capone, Hui Huang, Charles R. Sanders, Joshua A. Bauer, and Anne K. Kenworthy*

Cite This: *ACS Cent. Sci.* 2022, 8, 370–378

Read Online

ACCESS | Metrics & More | Article Recommendations | Supporting Information

ABSTRACT: Plasma membrane organization profoundly impacts cellular functionality. A well-known mechanism underlying this organization is through nanoscopic clustering of distinct lipids and proteins in membrane rafts. Despite their physiological importance, rafts remain a difficult-to-study aspect of membrane organization, in part because of the paucity of chemical tools to experimentally modulate their properties. Methods to selectively target rafts for therapeutic purposes are also currently lacking. To tackle these problems, we developed a high-throughput screen and an accompanying image analysis pipeline to identify small molecules that enhance or inhibit raft formation. Cell-derived giant plasma membrane vesicles were used as the experimental platform. A proof-of-principle screen using a bioactive lipid library demonstrates that this method is robust and capable of validating established raft modulators including C6- and C8-ceramide, miltefosine, and epigallocatechin gallate as well as identifying new ones. The platform we describe here represents a powerful tool to discover new chemical approaches to manipulate rafts and their components.

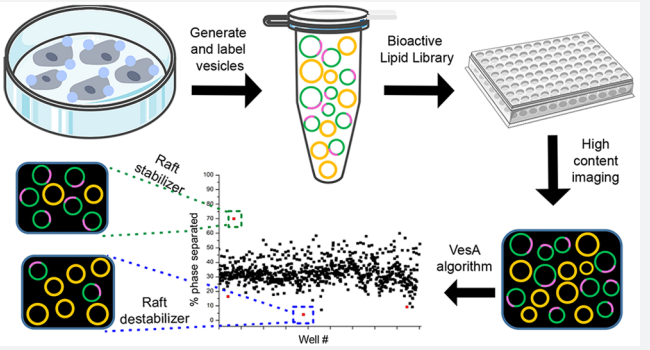

INTRODUCTION

Membrane rafts represent an extensively studied yet persistently enigmatic example of how membrane organization can modulate cellular function.[1] Typically defined as nanoscopic cholesterol-enriched domains that share properties with liquid ordered domains *in vitro*, rafts coexist with disordered domains in cell membranes and regulate numerous cellular functions by controlling the interaction partners and proximal membrane environment of associated proteins.[1] Consistent with their extensive biological roles, rafts have been implicated in a variety of normal physiological processes as well as pathological conditions.[1−6] Raft-dependent processes are typically identified and manipulated by altering membrane lipid composition, most commonly via cholesterol depletion.[1] However, such approaches can have significant pleiotropic effects and nonspecifically affect multiple lipid-dependent pathways.[7,8]

Another possible, though not yet widely explored, approach to modulate rafts in biological membranes is through the use of small molecules.[2−5,9] For example, specific therapeutics that can modulate microdomains are being actively considered for development.[5] Besides targeting specific lipids that alter receptor signaling, certain drugs can also modulate general properties of membrane rafts.[10,11] Furthermore, in cancer cell lines, changes in membrane heterogeneity are correlated with resistance to chemotherapeutics, and altering membrane heterogeneity can modulate cellular responses to chemotherapeutic drugs.[12] Thus, chemically based strategies could potentially provide new experimental tools to manipulate rafts *in vitro* and even eventually establish new therapeutics for human diseases linked to raft biology. To our knowledge, however, systematic screens to identify small molecules that target the formation and properties of rafts have not been described.

Major barriers to the discovery of small molecule modulators of rafts are that, in cells, rafts are diffraction-limited in size and are only transiently stable.[13] Thus, raft modulators need to be identified in model systems that allow for the visualization of large-scale domains while also retaining the complexity of cell membranes. Giant plasma membrane vesicles (GPMVs) offer an attractive solution to this problem.[8,14−16] Derived from the plasma membrane of adherent cells, these micron-scale blebs consist of a complex mixture of proteins and lipids reflective of

Received: August 31, 2021
Published: February 21, 2022

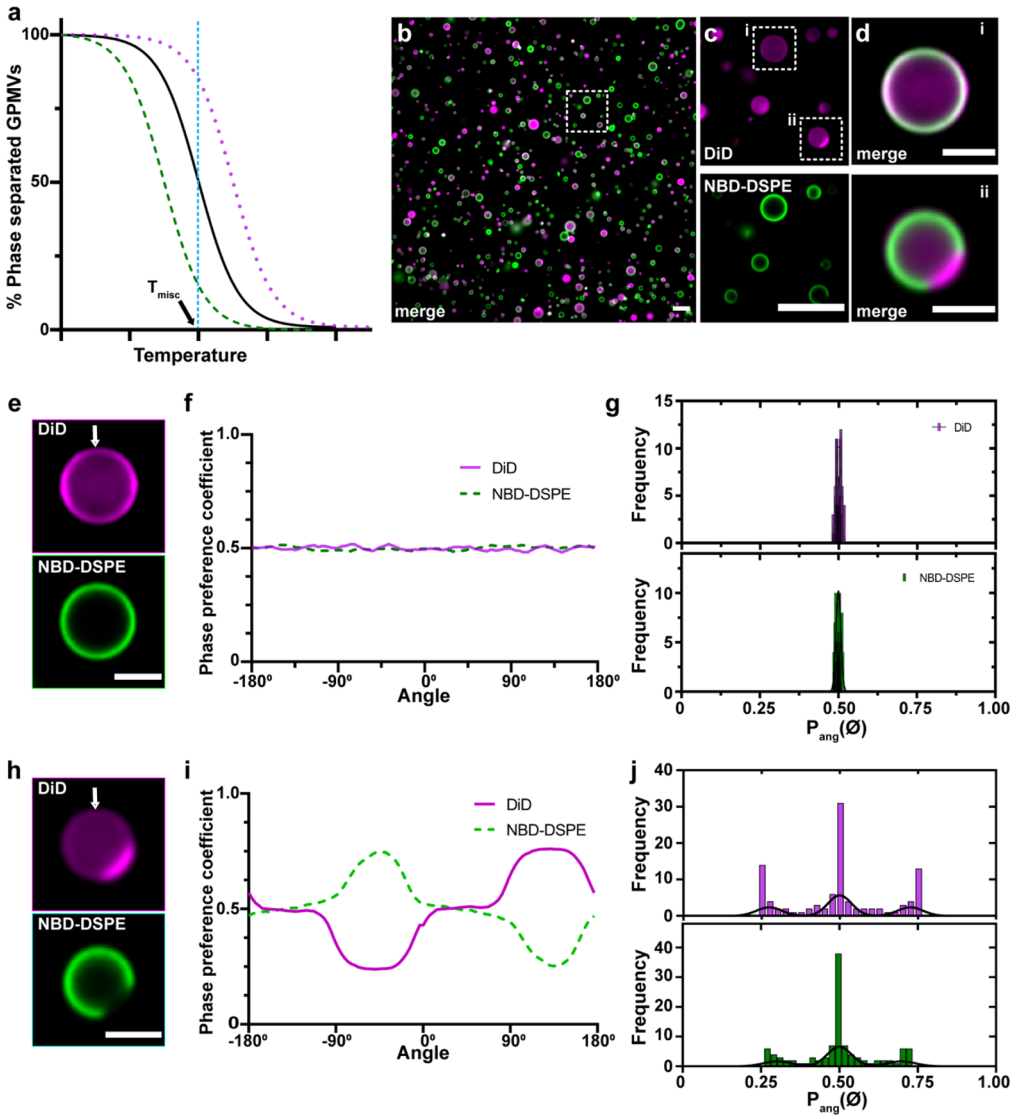

Figure 1. Principles underlying the high-content imaging screen and data analysis pipeline. (a) The addition of small molecules can hypothetically enhance (magenta line), impede (green line), or have no effect on (black line) the ability of GPMVs to undergo phase separation. These outcomes can be distinguished by comparing the percentage of phase-separated vesicles observed under control and experimental conditions at a single temperature (dotted blue line). (b–d) Representative high-content image of HeLa cell-derived GPMVs labeled with DiD (magenta) and NBD-DSPE (green) shown at increasingly higher magnifications. Scale bars: (b) 20 μm, (c) 20 μm, and (d) 5 μm. (e–j) Example of how angular phase preference coefficients $p_{ang}(\phi)$ are measured as a function of angle ϕ and used to discern single phase and phase-separated GPMVs. (e–g) Example of a single phase GPMV, together with a plot and histograms of its corresponding angular phase preference coefficients. (h–j) Example of a phase-separated GPMV, together with a plot and histograms of its angular phase preference coefficients. Scale bars (e, h): 5 μm.

the parent cell plasma membrane composition. A key feature of GPMVs is their ability to undergo temperature-dependent demixing that leads to the formation of coexisting macroscopic liquid raftlike and nonraft domains. These domains share features with liquid-ordered and liquid-disordered phases found in synthetic model membranes and can be labeled with phase-specific fluorescent dyes, allowing for their visualization using standard fluorescence microscopy approaches.[8,14−16] The temperature at which 50% of GPMVs are phase-separated under a given set of experimental conditions is defined as the miscibility transition temperature, T_{misc}. T_{misc} varies as a function of cell type and growth conditions and is hypothesized to reflect the size and lifetime of nanoscopic domains at physiological temperature.[17] Changes in T_{misc} have also been correlated to lipid order as measured by other analytical methods.[18−20] Thus, T_{misc} provides a simple and robust measure of raft stability.[21] T_{misc} is also sensitive to the effect of small molecules and bioactive compounds.[11,12,16,19,22,23] Here, we exploit this behavior to develop an unbiased, high-throughput screen (HTS) using GPMVs to identify new chemical modulators of rafts.

RESULTS

Conceptual Basis for the Screen. Classical measurements of T_{misc} are performed by measuring the percentage of phase-separated GPMVs using fluorescence microscopy as a function of temperature.[16] Effects of small molecules or other treatments on membrane phase behavior are then evaluated by comparing T_{misc} measurements obtained under each condition.[11,16,12,19,22−24] This approach is not practical for high-throughput screening applications, which typically are performed at a single temperature. We therefore chose to

https://doi.org/10.1021/acscentsci.1c01058
ACS Cent. Sci. 2022, 8, 370−378

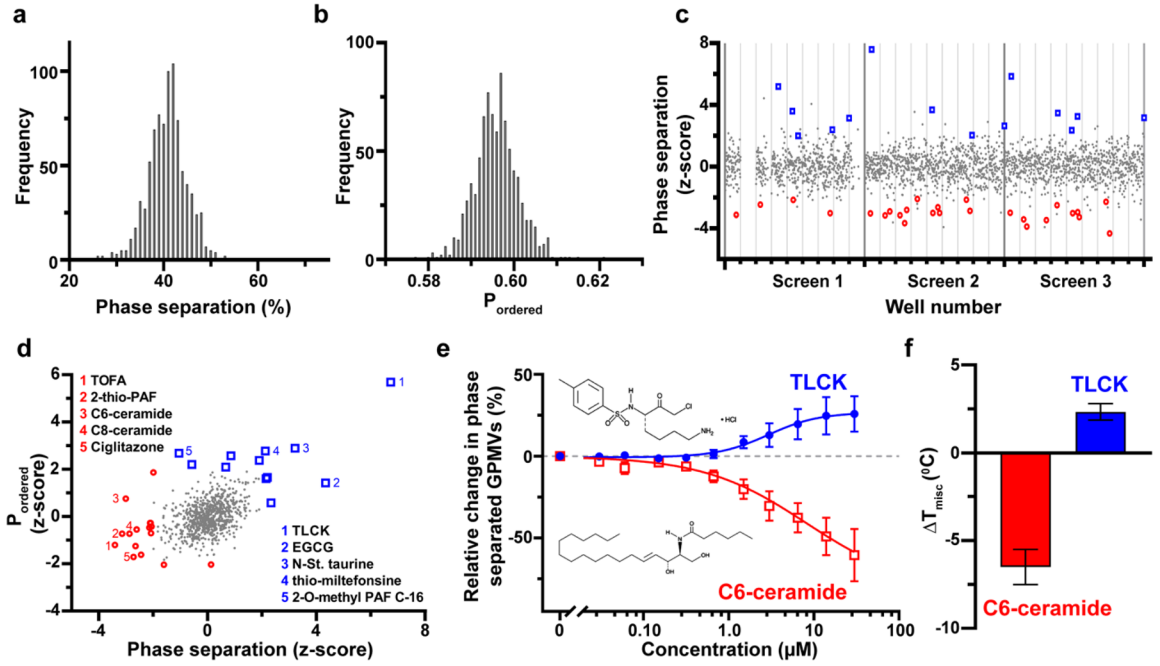

Figure 2. Results and validation of HTS for compounds that impact GPMV phase behavior. Histograms of (a) percent phase-separated vesicles and (b) $P_{ordered}$ for NBD-DSPE across all wells for one representative screen. (c) *Z*-scores for percentage of phase-separated vesicles across three independent screens performed on different days to test reproducibility. Vertical lines demarcate the position of individual plates in each screen. Each data point corresponds to measurements from an individual well (single compound). Compounds with *Z*-scores >2 are shown in blue, and compounds with Z-scores <−2 are shown in red. (d) Plot comparing the average Z-scores for $P_{ordered}$ of NBD-DSPE versus the average Z-scores for the percentage of phase-separated vesicles versus for each compound across all screens. The identities of several hits are indicated on the graph. (e) Dose−response curves for two representative hits, TLCK and C6-ceramide. Data represent the mean ± SD from 2 independent experiments performed in duplicate. Insets show structures of TLCK and C6-ceramide. (f) Impact of C6-ceramide and TLCK on ΔT_{misc}. See Figure S7 for examples of curves used to calculate ΔT_{misc}. Data represent the mean ± SD from 2 independent experiments. Abbreviations in panel d are as follows: TOFA, 5-(tetradecyloxy)-2-furancarboxylic acid; 2-thio-PAF, 1-*O*-hexadecyl-2-deoxy-2-thio-*S*-acetyl-sn-glyceryl-3-phosphorylcholine; TLCK, Nα-tosyl-L-lysyl chloromethyl ketone; EGCG, (−)-epigallocatecatchin gallate; N-St. taurine, N-stearoyl taurine; 2-*O*-methyl PAF 16, 1-*O*-hexadecyl-2-*O*-methyl-*sn*-glyceryl-3-phosphorylcholine.

monitor changes in the percentage of phase-separated GPMVs at a single temperature in response to the addition of small molecules as a surrogate for measuring T_{misc} directly (Figure 1a). This approach requires that a significant fraction of GPMVs are phase-separated under control conditions, such that experimentally induced changes can be readily detected. To fulfill this requirement, we used GPMVs isolated from HeLa cells, which are known to yield a significant fraction of phase-separated vesicles at room temperature.[25] Based on established criteria, compounds that increase the percentage of phase-separated GPMVs are defined as raft stabilizers, whereas those that decrease the percentage of phase-separated GPMVs function as raft disruptors/inhibitors of raft formation and lipid heterogeneity.[11,24]

To visualize phase separation, GPMVs were labeled with the fluorescent lipid NBD-DSPE to mark the raft phase and DiD to mark the nonraft phase.[15] In phase-separated vesicles, these markers are enriched in their preferred domains, such that a given vesicle contains a coexisting NBD-DSPE-rich phase and a DiD-rich phase. In contrast, NBD-DSPE and DiD colocalize in a single uniform phase in GPMVs that are not phase-separated. We also optimized conditions to isolate and plate GPMVs in multiwell plates. These modifications enabled us to capture images containing upward of hundreds of GPMVs per field at high resolution (Figure 1b−d), setting the stage for high-content imaging.

Development of an Automated Data Analysis Pipeline to Enable High-Content Imaging of GPMVs. We next established a pipeline for GPMV data analysis. To date, analyses of GPMVs have been performed manually,[15,16,26] but this approach is not feasible for high-content imaging. We developed a custom MATLAB-based pipeline to automate GPMV image analysis based on an algorithm that automatically detects and analyzes individual GPMVs in fluorescence images (see Figure S1 for an overview). It begins by identifying disc-shaped objects and excluding those that fail to meet certain selection criteria (Figure S2). The position of the membrane contour for each accepted vesicle is then mapped, and plots of fluorescence intensity along the vesicle membrane are generated (Figure S3).

The algorithm next uses the fluorescence intensity information in the red and green channels to calculate a metric $p_{ang}(\phi)$ that quantifies the preference of the fluorescent markers for the ordered and disordered phases as a function of angle ϕ around the vesicle perimeter. We refer to this metric as a phase preference coefficient $p_{ang}(\phi)$. It is defined as

$$p_{ang}(\phi) = \frac{I(\phi)}{I(\phi) + I(\phi + 180^\circ)}$$

Here, $I(\phi)$ corresponds to the fluorescence intensity at angle ϕ, and $I(\phi + 180^\circ)$ is the fluorescence intensity at angle $\phi + 180^\circ$. This analysis assumes that the fluorescence intensity at a particular position is proportional to dye concentration. Each GPMV is sampled at angles ranging from 0 to 180° and from 0 to −180°. In effect, this is the equivalent of drawing a line

https://doi.org/10.1021/acscentsci.1c01058
ACS Cent. Sci. 2022, 8, 370−378

Table 1. Compounds That Significantly Alter % Phase-Separated GPMVs

chemical name[a]	CasRn	effect on % phase-separated vesicles	*z*-score	ALogP	function[b]
TOFA	54857-86-2	↓	−3.41	6.85	noncytotoxic inhibitor of acetyl-CoA carboxylase and fatty acid synthesis
2-thio-PAF	96801-55-7	↓	−3.15	4.02	isoteric analogue of platelet activating factor
C6 ceramide (d18:1/6:0)	124753-97-5	↓	−3.01	6.88	cell permeable analogue of naturally occurring ceramide
C8 ceramide (d18:1/8:0)	74713-59-0	↓	−2.87	7.79	cell permeable ceramide analogue
ciglitazone	74772-77-3	↓	−2.73	4.53	antidiabetic drug; potent and selective PPARγ ligand
oleyl trifluoromethyl ketone	177987-23-4	↓	−2.65	8.05	analogue of oleic acid
OMDM-1	616884-62-9	↓	−2.62	7.59	endocannabinoid analogue; inhibitor of arachidonoyl ethanolamide uptake
cis-trismethoxy resveratrol	94608-23-8	↓	−2.45	3.77	antioxidant found in grapes and red wine with antiproliferative, antineoplastic, and antiangiogenic activities
11(Z),14(Z)-eicosadienoic acid	2091-39-6	↓	−2.15	7.33	uncommon naturally occurring polyunsaturated fatty acid
(2S)-OMPT	1217471-69-6	↓	−2.12	7.27	selective agonist of the lysophosphatidic acid 3 (LPA_3) receptor
O-1602	317321-41-8	↓	−2.10	4.79	abnormal cannabidiorcin; agonist of G-protein coupled receptor 55
N,*N*-dimethylsphingosine (d18:1)	119567-63-4	↓	−2.09	5.79	metabolite of sphingosine and an inhibitor of sphingosine kinase
SU6656	330161-87-0	↓	−2.06	2.62	selective inhibitor of Src kinases
PAF C-16	74389-68-7	↓	−2.00	3.46	platelet activating factor C-16; mediates neutrophil migration and reactive oxygen species production
TLCK hydrochloride	4238-41-9	↑	6.73	2.18	nonselective proteinase inhibitor
(−)-epigallocatechin gallate	989-51-5	↑	4.33	3.10	phenol found in green and black tea with diverse biological activities
N-stearoyl taurine	63155-80-6	↑	3.21	6.29	amino-acyl endocannabinoid
XAV939	284028-89-3	↑	2.33	3.68	tankyrase inhibitor
N-palmitoyl taurine	83982-06-3	↑	2.19	5.38	amino-acyl endocannabinoid
8-piperazin-1-yl-isoquinoline (hydrochloride)	936643-79-7	↑	2.14	1.17	synthetic intermediate used for pharmacological synthesis
thio-miltefosine	943022-11-5	↑	2.12	4.47	analogue of miltefosine, an inhibitor of phosphocholine cytidylyl transferase (CTP) with antimetastatic properties

[a]Abbreviations: TOFA, 5-(tetradecyloxy)-2-furancarboxylic acid; 2-thio-PAF, 1-*O*-hexadecyl-2-deoxy-2-thio-*S*-acetyl-sn-glyceryl-3-phosphorylcholine; OMDM-1, (S)-*N*-(1-(4-hydroxyphenyl)-2-hydroxyethyl) oleamide; (2S)-OMPT, 9Z-octadecenoic acid, (2S)-3-[(hydroxymercaptophosphinyl)oxy]-2-methoxypropyl ester, triethyl ammonium salt (1:2); O-1602, 5-methyl-4-[(1R,6R)-3-methyl-6-(1-methylethenyl)-2-cyclohexen-1-yl]-1,3-benzenediol; SU6656, 2,3-dihydro-*N*,*N*-dimethyl-2-oxo-3-[(4,5,6,7-tetrahydro-1*H*-indol-2-yl)methylene]-1*H*-indole-5-sulfonamide; PAF C-16, platelet activating factor C-16 or 1-*O*-hexadecyl-2-*O*-acetyl-sn-glyceryl-3-phosphorylcholine; TLCK= Nα-tosyl-Lys chloromethyl ketone; XAV939, 3,5,7,8-tetrahydro-2-[4-(trifluoromethyl)phenyl]-4*H*-thiopyrano[4,3-d]pyrimidin-4-one. [b]As reported in the Cayman product information.

profile bisecting the GPMV at each angle ϕ and using this information to calculate the percent of the dye present in the phase at angle ϕ. It is thus a generalized version of previously reported metrics reporting on the enrichment of fluorescent dyes or lipids in ordered domains such as % Lo, a measure of the preference of lipid probes for the Lo phase,[27] and % raft, a measure of the % of a given protein in the raft phase.[15] The main distinctions, for the $p_{ang}(\phi)$ measurement, are (i) that the analysis is performed for every GPMV, (ii) that the bisecting lines are placed at every angle and are not limited to lines that cross through two different phases, and (iii) that the analysis does not make an *a priori* assumption about which phase corresponds to the ordered or disordered domain.

For a GPMV in which a single phase is present, i.e., the distribution of red and green dye uniformly distributed across all angles, $p_{ang}(\phi)$ yields a value of 0.5 (Figure 1e−g). For a phase-separated GPMV, typically, three distinct $p_{ang}(\phi)$ values are obtained (Figure 1h−j). For angles where the line bisects the same phase at angles ϕ and ϕ + 180°, $p_{ang}(\phi)$ yields a value of 0.5. The other two values of $p_{ang}(\phi)$ report on the phase preference of the dye for the two distinct phases. When $I(\phi)$ corresponds to the brighter phase, $p_{ang}(\phi)$ will be >0.5. Conversely, when $I(\phi)$ corresponds to the dimmer phase, $p_{ang}(\phi)$ will be <0.5. Because each GPMV is sampled at angles ranging from 0 to 180° and from 0 to −180°, each position is sampled twice but from different directions (Figure 1h−j).

The program then generates histograms of $p_{ang}(\phi)$ for each GPMV and fits them to determine (i) if they are best described by one Gaussian (single phase) or three Gaussians (phase-separated) and (ii) the position of the maxima recorded. Each vesicle is then scored as phase-separated or not depending on whether histograms of the partition coefficients consist of a single peak, indicating that a single phase is present, or multiple peaks, reflecting the presence of fluorophore-rich and fluorophore-poor domains (Figure 1e−j). Using this tool, it is possible to quickly identify and analyze hundreds of individual GPMVs per image across multiple images and wells of multiwell plates in an automated fashion. This enabled us to quantify phase separation and phase preference coefficients for large vesicle populations, for example, by averaging the percentage of phase-separated vesicles and NBD-DSPE phase preference for the GPMVs detected in each well and then generating histograms of these values across all of the wells of a representative screen (Figure 2a,b).

Because the data analysis pipeline depends on the accurate detection of the percentage of phase-separated vesicles, we next confirmed whether it could detect phase-separated vesicles with equal efficiency in the red and green channels

https://doi.org/10.1021/acscentsci.1c01058
ACS Cent. Sci. 2022, 8, 370−378

Table 2. Compounds That Significantly Alter NBD-DSPE Raft Phase Preference

chemical name[a]	CasRn	effect on $p_{ang}(\phi)$	z-score	ALogP	function[b]
CAY10444	298186-80-8	↓	−2.04	2.05	selective antagonist of the $S1P_3$/EDG3 receptor, a member of a family of G-protein coupled receptors that bind sphingosine-1 phosphate (S1P)
FR122047 (hydrochloride)	130717-51-0	↓	−2.03	3.79	selective inhibitor of COX-1
TLCK hydrochloride	4238-41-9	↑	5.69	2.18	nonselective proteinase inhibitor
N-stearoyl taurine	63155-80-6	↑	2.89	6.29	amino-acyl endocannabinoid
thio-miltefosine	943022-11-5	↑	2.78	4.47	analogue of miltefosine, an inhibitor of phosphocholine cytidylyl transferase (CTP) with antimetastatic properties
2-*O*-methyl PAF C-16	78858-44-3	↑	2.68	3.49	synthetic platelet activating factor analogue
S-ethyl isothiourea (hydrobromide)	1071-37-0	↑	2.57	0.77	potent inhibitor of nitric oxide synthase
arachidonoyl-2′-fluoroethylamide	166100-37-4	↑	2.38	6.88	analogue of anandamide that binds cannabinoid receptors
methylcarbamyl PAF C-16	91575-58-5	↑	2.20	3.46	stable analogue of platelet activating factor C-16
MK-886	118414-82-7	↑	2.10	8.11	amino-acyl endocannabinoid

[a]Abbreviations: 2CAY10444, 2-undecyl-thiazolidine-4-carboxylic acid; FR122047, 1-[[4,5-bis(4-methoxyphenyl)-2-thiazolyl]carbonyl]-4-methyl-piperazine, monohydrochloride; MK-886, 1-[(4-chlorophenyl)methyl]-3-[(1,1-dimethylethyl)thio]-α,α-dimethyl-5-(1-methylethyl)-1*H*-indole-2-propanoic acid. [b]As reported in the Cayman product information.

across multiple images (Table S1). For GPMVs that contain both red and green dyes, ∼90% were reported as being phase-separated in the red channel, compared to ∼65% reported as phase-separated in the green channel. This is due to the exclusion of a large percentage of red GPMVs from the final analysis, likely due to the relatively high level of DiD fluorescence in the lumen compared to the membrane contour (Figure S2c). This appears to be a consequence of the wide field imaging approach used in the high-content imaging microscope, as we found that if GPMVs were imaged using a confocal microscope, a similar percentage of vesicles were identified as phase-separated in both the red and green channels (Figure S4). Given this systematic underdetection of the vesicles in the DiD channel, only data from the green channel (NBD-DSPE) were used for subsequent data analyses of % phase-separated vesicles and $p_{ang}(\phi)$. Because NBD-DSPE is a raft-preferring lipid probe, we report values of $p_{ang}(\phi) > 0.5$, which reflect its enrichment in the ordered phase. For simplicity, we will subsequently refer to this as $P_{ordered}$. $P_{ordered}$ is essentially the equivalent of the previously reported % Lo metric.[27] In particular, % Lo = $F_{Lo}/(F_{Lo} + F_{Ld})$, where F_{Lo} and F_{Ld} are the fluorescence intensities of the reporter in the raft and nonraft phase, respectively.[27]

A Proof-of-Principle Screen Identifies Established and New Chemical Modulators of Rafts. To provide a proof of concept, we screened the Cayman lipid library containing ∼850 bioactive lipidlike compounds in the Vanderbilt High-Throughput Screening Facility, using a 1 μM concentration of each compound across three independent screens. All screens were carried out using an automated microscope/high-content imaging system and robotic plate handler at room temperature (RT). After applying vesicle selection criteria, our final analysis was performed on $\sim 2 \times 10^6$ GPMVs, corresponding to an average of 868 ± 437 vesicles per compound. Compounds were initially scored based on their capacity to alter the percentage of phase-separated vesicles (Figure 2a). Seven compounds were found to significantly increase the percentage of phase-separated vesicles (z-score > 2) while 14 compounds decreased the percentage of phase-separated GPMVs across at least two independent screening trials (Table 1, Table S2). Consistent with previous reports,[28,29] short-chain ceramide analogues were consistently identified as raft disruptors that decreased the percentage of phase-separated vesicles. Acylated taurines were among the candidates that increased the percentage of phase-separated vesicles, i.e., stabilized rafts. We also identified a protease inhibitor, tosyl-L-lysyl-chloromethane hydrochloride (TLCK), as a potent raft stabilizer in the GPMV model.

Since the raft phase preference of lipid probes is known to be sensitive to the physical properties of membrane phases,[27] we also examined whether these are affected by the compounds. Ten compounds significantly altered the phase preference of NBD-DSPE (z-score > 2) (Figure 2b,d; Table 2, Table S2). Of the 850 compounds screened, three compounds (TLCK hydrochloride, *N*-stearoyl taurine, and thio-miltefosine) significantly affected both the percentage of phase-separated vesicles and the phase preference, while the others compounds affected only one parameter or the other (Tables 1 and 2, Table S1). Together, these results indicate that some but not all bioactive lipids modulate membrane phase behavior, with varying modes of action.

To validate the results of the screens, we selected two hits for deeper analysis: the short-chain ceramide analogue C6-ceramide and the protease inhibitor TLCK (Figure 2e,f). In dose−response assays, using freshly made reordered stocks of each compound, TLCK systematically increased the percentage of phase-separated vesicles as a function of increasing concentration, while the opposite effect was observed for increasing concentrations of C6-ceramide (Figure 2e). Their effects on the phase preference of NBD-DSPE were also dose-dependent (Figure S5). In contrast, the vehicle DMSO had little effect on the percentage of phase-separated vesicles or phase preference except at the highest concentration studied (Figure S6).

Next, we independently validated the two candidates, TLCK and C6-ceramide, by determining changes in T_{misc} relative to DMSO. For these experiments, the percentage of phase-separated vesicles was measured as a function of temperature.[16] As expected, TLCK increased T_{misc}, whereas C6-ceramide lowered T_{misc} (Figure 2f, Figure S7). We also assessed their effects in several different cell types (Figure S8). Thus, these

https://doi.org/10.1021/acscentsci.1c01058
ACS Cent. Sci. 2022, 8, 370−378

compounds represent *bona fide* examples of raft modulators in the GPMV model.

SSMD* Metric Establishes the High-Content Imaging Screen As a Robust Tool to Identify New Raft Modulators. Finally, we used C6 ceramide and TLCK as positive controls to assess the quality and reproducibility of our assay. The use of the percentage of phase-separated vesicles as our metric restricts the dynamic range and the use of standard HTS assay metrics, such as Z-prime.[30,31] We therefore chose to calculate the robust strictly standardized mean difference (SSMD*) to evaluate assay performance and quality for HTS. This metric uses medians and median absolute deviations to estimate effect size and variability.[32,33] Based on their effects on the percentage of phase-separated GPMVs, we obtained SSMD* values of 8.84 ± 2.65 for C6 ceramide and 1.34 ± 0.29 for TLCK (mean ± SD, n = 3) (Figure S9), corresponding to extremely strong and moderate effects, respectively.[33] The SSMD* measurements thus confirm the robustness of the assay for HTS readiness and establish C6 ceramide and TLCK as useful positive controls for future screens.

DISCUSSION

In this work, we have provided a proof of concept for a high-throughput method to discover chemical modulators of membrane rafts. In addition to short-chain ceramides, several of the bioactive lipids identified here, including the polyphenols epigallocatechin gallate and resveratrol as well as the alkylphospholipid analogue miltefosine, have previously been identified as raft modulators, demonstrating the validity and robust nature of our approach.[9,28,29,34−39] Importantly, however, we also identified compounds that to our knowledge have not previously been shown to act on rafts in model membrane systems or cells, such as TLCK.

The hits varied in their impact on membranes. Some enhanced while others inhibited membrane phase separation. The hits thus include examples of compounds that stabilize raft formation as well as some that inhibit raft formation. Some compounds affected both phase separation and lipid probe phase preference, suggesting that they simultaneously affect lipid raft composition and behavior. Looking broadly across the hits, no overall trends relating charge or lipophilicity as reported as ALogP values (a method used to estimate the logarithm of the partition coefficient P of compounds in octanol/water[40,41]) to activity were immediately evident (Figures S10 and S11, Tables 1 and 2). However, the compounds that resulted in the strongest decreases in phase separation trended toward higher ALogP values compared to those that show a corresponding increase (Figure S10, Table 1). Not surprisingly, based on the composition of the bioactive lipid library, a bulk of the hit compounds have molecular architectures similar to fatty acids.

Together, these findings suggest that at least a subset of the hits impact domain formation by preferentially inserting into either the ordered or disordered phase, leading to changes in their physical properties and ultimately their miscibility. However, it is also possible that some of the hits influence membrane phase separation in other ways. For example, some of the non-fatty-acid singleton hits, such as (−)-epigallocatechin, TLCK, resveratrol, and ciglitazone, contain chemical moieties that have been recognized to commonly yield false-positive screening results and/or are known to exhibit pleiotropic biological effects, including cell membrane perturbations.[42,43] Some compounds could potentially impact phase behavior indirectly by chemically modifying lipids or membrane proteins, similar to the behavior of some of the chemicals used to induce blebbing of GPMVs.[20] It is possible, for example, that TLCK, which contains an electrophilic group, can covalently attach itself to some component of the membrane and thus induce the observed effects. Further testing which of these mechanisms are operative for each of these compounds as well as evaluating their impact on raft-dependent biological activities are important goals for the future.

It is also important to recognize the limitations of this assay in identifying viable raft targets. Some of these limitations are technical. For example, we observed positional effects that are likely linked to temperature changes as the plates were loaded into the imaging chamber, an effect that could be corrected computationally. We also found that our data analysis algorithm underestimates the percentage of GPMVs labeled with DiD due to the fluorescence signal in the interior of the GPMVs. We overcame this issue by relying on the NBD-DSPE fluorescence signal for data analysis and showed that this effect can also be minimized experimentally using confocal imaging. Because the assay was carried out at RT, only the DTT method for isolating GPMVs can be used. This is because the transition temperature of GPMVs isolated using the NEM method is quite low.[20] Indeed, at RT, using the NEM method, nearly all of our GPMVs exhibit a single phase (data not shown). It is also important to optimize the parameters used in the high-content image analysis software for different experimental set-ups and to visually inspect images during this process. Other limitations of the assay reflect the imperfect nature of GPMVs as a proxy for quantifying lipid raft properties. Although they have a lipid composition similar to plasma membranes, GPMVs exhibit a partial loss of lipid asymmetry.[15] They also lack an underlying actin cytoskeleton, which normally functions to corral membrane domains and sustain or dampen lipid-mediated heterogeneity.[44−46] Membrane curvature also differs between GPMVs and live cell membranes. Clearly, much work remains to determine whether the compounds identified here modulate raft-mediated functions in cells such as clathrin-independent endocytosis or immune signaling.[47,48] Establishing whether their raft-modulating activities in GPMVs are predictive—or not—of their biological consequences should help lead to a better understanding of the limitations of the raft hypothesis itself.

We envision a number of immediate applications of this screening approach beyond extending it to other chemical libraries. As one example, it could be used to identify small molecules capable of modulating rafts without requiring changing levels of membrane cholesterol or sphingolipids, the current standard in the field. Since many clinically relevant membrane processes occur on the inner leaflet of the plasma membrane, this approach could be expanded to identify small molecules that act on inner leaflet phase separation using lipidated raft and nonraft preferring proteins as markers.[47] Examples of a disordered domain marker include a peptide anchored to the inner leaflet through a polybasic sequence and an attached geranylgeranyl moiety, whereas a minimal lipidated peptide with a saturated palmitoyl and myristoyl modifications preferentially associates with ordered domains.[14,47,49] Given that rafts have been broadly implicated in human disease and are also exploited by pathogens,[1−6] candidates discovered through this approach could also be utilized to probe the pathophysiology of raft-associated diseases and possibly even

https://doi.org/10.1021/acscentsci.1c01058
ACS Cent. Sci. 2022, 8, 370−378

be exploited for therapeutic applications. Our screening strategy could also be leveraged to identify small molecules that modulate the association of specific proteins with raftlike domains while leaving rafts themselves unperturbed. Finally, the high-content image analysis pipeline described here should also have broad and immediate applications in studies utilizing GPMVs and other vesicle-based membrane models such as GUVs. For example, it could greatly accelerate efforts to understand mechanisms that control the affinity of membrane proteins for raft domains.[26] Through these combined advances, it should become feasible to study, manipulate, and harness rafts in ways not previously possible.

■ ASSOCIATED CONTENT

Supporting Information

The Supporting Information is available free of charge at https://pubs.acs.org/doi/10.1021/acscentsci.1c01058.

Methods; quantification of the efficiency of detection of phase-separated GPMVs using DiD fluorescence versus NBD-DSPE fluorescence across screens; metrics for the hits; a representative figure illustrating the automated vesicle selection process; a description of contour detection and refinement of membrane position of individual GPMVs; an analysis of the percentage of phase-separated vesicles detected in the DiD and NBD-DSPE channels using wide field versus confocal imaging; a dose−response curve showing the effects of TLCK and C6-ceramide on $P_{ordered}$ for NBD-DSPE; dose−response curves showing the effects of DMSO on the percentage of phase-separated vesicles and $P_{ordered}$ for NBD-DSPE; a representative temperature scan illustrating the effect of TLCK on T_{misc}; quantification of the effects of TLCK and C6-ceramide on GPMVs isolated from several different cell lines; results of experiments designed to test the HTS assay robustness based on SSMD* calculations; chemical structures of hits from the bioactivity lipid library that impact the percentage of phase-separated GPMVs; chemical structures of hits from the bioactivity lipid library that impact $P_{ordered}$ for NBD-DSPE; a description of how phase-separated GPMVs are identified using the "colocalization" approach; an overview of approaches used to correct for positional effects and calculate *Z*-scores; and a userguide describing the functionality of the VesA software (PDF)

■ AUTHOR INFORMATION

Corresponding Author

Anne K. Kenworthy − *Department of Molecular Physiology and Biophysics, Vanderbilt School of Medicine, Nashville, Tennessee 37232, United States;* Present Address: N.F., A.T., A.K.K.: Center for Membrane and Cell Physiology and Department of Molecular Physiology and Biological Physics, University of Virginia School of Medicine, Charlottesville, VA 22903, USA; orcid.org/0000-0001-6567-9059; Email: akk7hp@virginia.edu

Authors

Nico Fricke − *Department of Molecular Physiology and Biophysics, Vanderbilt School of Medicine, Nashville, Tennessee 37232, United States;* Present Address: N.F., A.T., A.K.K.: Center for Membrane and Cell Physiology and Department of Molecular Physiology and Biological Physics, University of Virginia School of Medicine, Charlottesville, VA 22903, USA

Krishnan Raghunathan − *Department of Molecular Physiology and Biophysics, Vanderbilt School of Medicine, Nashville, Tennessee 37232, United States;* Present Address: K.R.: Department of Pediatrics, University of Pittsburgh, Pittsburgh, PA 15224, USA; orcid.org/0000-0003-2228-6313

Ajit Tiwari − *Department of Molecular Physiology and Biophysics, Vanderbilt School of Medicine, Nashville, Tennessee 37232, United States;* Present Address: N.F., A.T., A.K.K.: Center for Membrane and Cell Physiology and Department of Molecular Physiology and Biological Physics, University of Virginia School of Medicine, Charlottesville, VA 22903, USA

Katherine M. Stefanski − *Department of Biochemistry, Vanderbilt School of Medicine, Nashville, Tennessee 37240, United States*

Muthuraj Balakrishnan − *Center for Membrane and Cell Physiology and Department of Molecular Physiology and Biological Physics, University of Virginia School of Medicine, Charlottesville, Virginia 22903, United States*

Alex G. Waterson − *Department of Pharmacology, Vanderbilt School of Medicine, Nashville, Tennessee 37232, United States*

Ricardo Capone − *Department of Molecular Physiology and Biophysics, Vanderbilt School of Medicine, Nashville, Tennessee 37232, United States;* Present Address: R.C.: Department of Biochemistry, Vanderbilt School of Medicine, Nashville, TN 37240, USA

Hui Huang − *Department of Biochemistry, Vanderbilt School of Medicine, Nashville, Tennessee 37240, United States*

Charles R. Sanders − *Department of Biochemistry, Vanderbilt School of Medicine, Nashville, Tennessee 37240, United States;* orcid.org/0000-0003-2046-2862

Joshua A. Bauer − *Department of Biochemistry, Vanderbilt School of Medicine, Nashville, Tennessee 37240, United States; Vanderbilt Institute of Chemical Biology, High-Throughput Screening Facility, Vanderbilt School of Medicine, Nashville, Tennessee 37232, United States*

Complete contact information is available at: https://pubs.acs.org/10.1021/acscentsci.1c01058

Author Contributions

[¶]N.F., K.R., and A.T. contributed equally to this work.

Notes

The authors declare no competing financial interest.

■ ACKNOWLEDGMENTS

We thank Drs. Ilya Levental and Kandice Levental and members of the Kenworthy lab for feedback on the manuscript and Dr. Abbie Neininger for assistance with troubleshooting the MATLAB code. This work was supported by NIH 1RF1 AG056147, NIH R01 GM138493, NIH R01 GM106720, NIH grant S10 OD021723 (Operetta), and a Vanderbilt Stanley Cohen Award. K.M.S. was supported by NIH training grant T32 NS007491. J.A.B. was supported by an NCI R50 award R50 CA211206. Experiments were performed in the Vanderbilt High-Throughput Screening (HTS) Core Facility with assistance provided by Corbin Whitwell and Paige Vinson. The HTS Core receives support from the Vanderbilt

Institute of Chemical Biology and the Vanderbilt Ingram Cancer Center (P30 CA68485). The Cayman Lipid Library was distributed by the Vanderbilt High-Throughput Screening Core Facility. The content is solely the responsibility of the authors and does not necessarily represent the official views of the National Institutes of Health.

REFERENCES

(1) Sezgin, E.; Levental, I.; Mayor, S.; Eggeling, C. The mystery of membrane organization: Composition, regulation and roles of lipid rafts. *Nat Rev Mol Cell Biol* **2017**, *18* (6), 361−374.
(2) Verma, S. P. HIV: A raft-targeting approach for prevention and therapy using plant-derived compounds (review). *Curr Drug Targets* **2009**, *10* (1), 51−9.
(3) Hryniewicz-Jankowska, A.; Augoff, K.; Biernatowska, A.; Podkalicka, J.; Sikorski, A. F. Membrane rafts as a novel target in cancer therapy. *Biochim. Biophys. Acta* **2014**, *1845* (2), 155−65.
(4) Bernardes, N.; Fialho, A. M. Perturbing the dynamics and organization of cell membrane components: A new paradigm for cancer-targeted therapies. *Int J Mol Sci* **2018**, *19* (12), 3871.
(5) Sviridov, D.; Mukhamedova, N.; Miller, Y. I. Lipid rafts as a therapeutic target. *J. Lipid Res.* **2020**, *61* (5), 687−695.
(6) Bukrinsky, M. I.; Mukhamedova, N.; Sviridov, D. Lipid rafts and pathogens: The art of deception and exploitation. *J. Lipid Res.* **2020**, *61* (5), 601−610.
(7) Zidovetzki, R.; Levitan, I. Use of cyclodextrins to manipulate plasma membrane cholesterol content: Evidence, misconceptions and control strategies. *Biochim. Biophys. Acta* **2007**, *1768* (6), 1311−24.
(8) Levental, K. R.; Levental, I. Giant plasma membrane vesicles: Models for understanding membrane organization. *Curr Top Membr* **2015**, *75*, 25−57.
(9) Tsuchiya, H.; Mizogami, M. Interaction of drugs with lipid raft membrane domains as a possible target. *Drug Target Insights* **2020**, *14*, 34−47.
(10) Zhou, Y.; Cho, K. J.; Plowman, S. J.; Hancock, J. F. Nonsteroidal anti-inflammatory drugs alter the spatiotemporal organization of Ras proteins on the plasma membrane. *J. Biol. Chem.* **2012**, *287* (20), 16586−95.
(11) Gray, E.; Karslake, J.; Machta, B. B.; Veatch, S. L. Liquid general anesthetics lower critical temperatures in plasma membrane vesicles. *Biophys. J.* **2013**, *105* (12), 2751−9.
(12) Raghunathan, K.; Ahsan, A.; Ray, D.; Nyati, M. K.; Veatch, S. L. Membrane transition temperature determines cisplatin response. *PLoS One* **2015**, *10* (10), e0140925.
(13) Levental, I.; Levental, K. R.; Heberle, F. A. Lipid rafts: Controversies resolved, mysteries remain. *Trends Cell Biol* **2020**, *30* (5), 341−353.
(14) Baumgart, T.; Hammond, A. T.; Sengupta, P.; Hess, S. T.; Holowka, D. A.; Baird, B. A.; Webb, W. W. Large-scale fluid/fluid phase separation of proteins and lipids in giant plasma membrane vesicles. *Proc Natl Acad Sci U S A* **2007**, *104* (9), 3165−70.
(15) Sezgin, E.; Kaiser, H. J.; Baumgart, T.; Schwille, P.; Simons, K.; Levental, I. Elucidating membrane structure and protein behavior using giant plasma membrane vesicles. *Nat Protoc* **2012**, *7* (6), 1042−51.
(16) Gerstle, Z.; Desai, R.; Veatch, S. L. Giant plasma membrane vesicles: An experimental tool for probing the effects of drugs and other conditions on membrane domain stability. *Methods Enzymol* **2018**, *603*, 129−150.
(17) Veatch, S. L.; Cicuta, P.; Sengupta, P.; Honerkamp-Smith, A.; Holowka, D.; Baird, B. Critical fluctuations in plasma membrane vesicles. *ACS Chem Biol* **2008**, *3* (5), 287−93.
(18) Podkalicka, J.; Biernatowska, A.; Majkowski, M.; Grzybek, M.; Sikorski, A. F. MPP1 as a factor regulating phase separation in giant plasma membrane-derived vesicles. *Biophys. J.* **2015**, *108* (9), 2201−11.
(19) Cornell, C. E.; McCarthy, N. L. C.; Levental, K. R.; Levental, I.; Brooks, N. J.; Keller, S. L. n-Alcohol length governs shift in Lo-Ld mixing temperatures in synthetic and cell-derived membranes. *Biophys. J.* **2017**, *113*, 1200−1211.
(20) Levental, I.; Grzybek, M.; Simons, K. Raft domains of variable properties and compositions in plasma membrane vesicles. *Proc Natl Acad Sci U S A* **2011**, *108* (28), 11411−6.
(21) Miller, E. J.; Ratajczak, A. M.; Anthony, A. A.; Mottau, M.; Rivera Gonzalez, X. I.; Honerkamp-Smith, A. R. Divide and conquer: How phase separation contributes to lateral transport and organization of membrane proteins and lipids. *Chem Phys Lipids* **2020**, *233*, 104985.
(22) Zhou, Y.; Maxwell, K. N.; Sezgin, E.; Lu, M.; Liang, H.; Hancock, J. F.; Dial, E. J.; Lichtenberger, L. M.; Levental, I. Bile acids modulate signaling by functional perturbation of plasma membrane domains. *J. Biol. Chem.* **2013**, *288* (50), 35660−70.
(23) Machta, B. B.; Gray, E.; Nouri, M.; McCarthy, N. L. C.; Gray, E. M.; Miller, A. L.; Brooks, N. J.; Veatch, S. L. Conditions that stabilize membrane domains also antagonize n-alcohol anesthesia. *Biophys. J.* **2016**, *111* (3), 537−545.
(24) Levental, K. R.; Lorent, J. H.; Lin, X.; Skinkle, A. D.; Surma, M. A.; Stockenbojer, E. A.; Gorfe, A. A.; Levental, I. Polyunsaturated lipids regulate membrane domain stability by tuning membrane order. *Biophys. J.* **2016**, *110* (8), 1800−10.
(25) Johnson, S. A.; Stinson, B. M.; Go, M. S.; Carmona, L. M.; Reminick, J. I.; Fang, X.; Baumgart, T. Temperature-dependent phase behavior and protein partitioning in giant plasma membrane vesicles. *Biochim. Biophys. Acta* **2010**, *1798* (7), 1427−35.
(26) Lorent, J. H.; Diaz-Rohrer, B.; Lin, X.; Spring, K.; Gorfe, A. A.; Levental, K. R.; Levental, I. Structural determinants and functional consequences of protein affinity for membrane rafts. *Nat Commun* **2017**, *8* (1), 1219.
(27) Sezgin, E.; Levental, I.; Grzybek, M.; Schwarzmann, G.; Mueller, V.; Honigmann, A.; Belov, V. N.; Eggeling, C.; Coskun, U.; Simons, K.; Schwille, P. Partitioning, diffusion, and ligand binding of raft lipid analogs in model and cellular plasma membranes. *Biochim. Biophys. Acta* **2012**, *1818* (7), 1777−84.
(28) Holowka, D.; Thanapuasuwan, K.; Baird, B. Short chain ceramides disrupt immunoreceptor signaling by inhibiting segregation of Lo from Ld Plasma membrane components. *Biol Open* **2018**, *7* (9), bio034702.
(29) Chiantia, S.; Kahya, N.; Schwille, P. Raft domain reorganization driven by short- and long-chain ceramide: a combined AFM and FCS study. *Langmuir* **2007**, *23*, 7659−7665.
(30) Zhang, J. H.; Chung, T. D.; Oldenburg, K. R. A simple statistical parameter for use in evaluation and validation of high throughput screening assays. *J Biomol Screen* **1999**, *4* (2), 67−73.
(31) Inglese, J.; Johnson, R. L.; Simeonov, A.; Xia, M.; Zheng, W.; Austin, C. P.; Auld, D. S. High-throughput screening assays for the identification of chemical probes. *Nat Chem Biol* **2007**, *3* (8), 466−79.
(32) Zhang, X. D. A pair of new statistical parameters for quality control in RNA interference high-throughput screening assays. *Genomics* **2007**, *89* (4), 552−61.
(33) Zhang, X. D. Illustration of SSMD, z score, SSMD*, z* score, and t statistic for hit selection in RNAi high-throughput screens. *J Biomol Screen* **2011**, *16* (7), 775−85.
(34) Adachi, S.; Nagao, T.; Ingolfsson, H. I.; Maxfield, F. R.; Andersen, O. S.; Kopelovich, L.; Weinstein, I. B. The inhibitory effect of (-)-epigallocatechin gallate on activation of the epidermal growth factor receptor is associated with altered lipid order in HT29 colon cancer cells. *Cancer Res.* **2007**, *67* (13), 6493−501.
(35) Duran, J. M.; Campelo, F.; van Galen, J.; Sachsenheimer, T.; Sot, J.; Egorov, M. V.; Rentero, C.; Enrich, C.; Polishchuk, R. S.; Goni, F. M.; Brugger, B.; Wieland, F.; Malhotra, V. Sphingomyelin organization is required for vesicle biogenesis at the Golgi complex. *EMBO J.* **2012**, *31* (24), 4535−46.
(36) Neves, A. R.; Nunes, C.; Amenitsch, H.; Reis, S. Resveratrol interaction with lipid bilayers: a synchrotron X-ray scattering study. *Langmuir* **2016**, *32* (48), 12914−12922.

https://doi.org/10.1021/acscentsci.1c01058
ACS Cent. Sci. 2022, 8, 370−378

(37) Neves, A. R.; Nunes, C.; Reis, S. Resveratrol induces ordered domains formation in biomembranes: Implication for its pleiotropic action. *Biochim. Biophys. Acta* **2016**, *1858* (1), 12−8.
(38) Heczkova, B.; Slotte, J. P. Effect of anti-tumor ether lipids on ordered domains in model membranes. *FEBS Lett.* **2006**, *580* (10), 2471−6.
(39) Zaremberg, V.; Ganesan, S.; Mahadeo, M. Lipids and membrane microdomains: The glycerolipid and alkylphosphocholine class of cancer chemotherapeutic drugs. *Handb Exp Pharmacol* **2019**, *259*, 261−288.
(40) Ghose, A. K.; Crippen, G. M. Atomic physicochemical parameters for 3-dimensional structure-directed quantitative structure-activity-relationships. 1. Partition-coefficients as a measure of hydrophobicity. *J. Comput. Chem.* **1986**, *7* (4), 565−577.
(41) Pyka, A.; Babuska, M.; Zachariasz, M. A comparison of theoretical methods of calculation of partition coefficients for selected drugs. *Acta Pol. Pharm.* **2006**, *63* (3), 159−167.
(42) Ingolfsson, H. I.; Thakur, P.; Herold, K. F.; Hobart, E. A.; Ramsey, N. B.; Periole, X.; de Jong, D. H.; Zwama, M.; Yilmaz, D.; Hall, K.; Maretzky, T.; Hemmings, H. C., Jr.; Blobel, C.; Marrink, S. J.; Kocer, A.; Sack, J. T.; Andersen, O. S. Phytochemicals perturb membranes and promiscuously alter protein function. *ACS Chem Biol* **2014**, *9* (8), 1788−98.
(43) Baell, J. B.; Holloway, G. A. New substructure filters for removal of pan assay interference compounds (PAINS) from screening libraries and for their exclusion in bioassays. *J. Med. Chem.* **2010**, *53* (7), 2719−40.
(44) Honigmann, A.; Sadeghi, S.; Keller, J.; Hell, S. W.; Eggeling, C.; Vink, R. A lipid bound actin meshwork organizes liquid phase separation in model membranes. *Elife* **2014**, *3*, e01671.
(45) Chichili, G. R.; Rodgers, W. Cytoskeleton-membrane interactions in membrane raft structure. *Cell. Mol. Life Sci.* **2009**, *66* (14), 2319−28.
(46) Lietha, D.; Izard, T. Roles of membrane domains in integrin-mediated cell adhesion. *Int J Mol Sci* **2020**, *21* (15), 5531.
(47) Stone, M. B.; Shelby, S. A.; Nunez, M. F.; Wisser, K.; Veatch, S. L. Protein sorting by lipid phase-like domains supports emergent signaling function in B lymphocyte plasma membranes. *Elife* **2017**, *6*, 19891.
(48) Verma, D. K.; Gupta, D.; Lal, S. K. Host lipid rafts play a major role in binding and endocytosis of Influenza A virus. *Viruses* **2018**, *10* (11), 650.
(49) Pyenta, P. S.; Holowka, D.; Baird, B. Cross-correlation analysis of inner-leaflet-anchored green fluorescent protein co-redistributed with IgE receptors and outer leaflet lipid raft components. *Biophys. J.* **2001**, *80*, 2120−2132.

https://doi.org/10.1021/acscentsci.1c01058
ACS Cent. Sci. 2022, 8, 370−378